Structural Eng./Earthquake Eng. Vol. 8, No. 3, 123s—129s, October 1991
Japan Society of Civil Engineers (Proc. of JSCE No. 437/I—17)

SEMI-UNIFIED CONSTITUTIVE MODEL FOR ELASTIC VISCOPLASTIC MATERIAL AT HIGH TEMPERATURES

SYED Saeed Ahmad* and
Shunsuke BABA**

Semi-unified constitutive equations are proposed for use in the analysis of rate and time dependent deformation of structural steel SS 41, at high temperatures. The material is assumed to behave as an elastic viscoplastic material. The effect of creep is introduced as contraction of yield surface, at each step of loading. Material parameters for the model can be obtained from standard creep and tension compression tests. Experiments have been performed on SS 41 steel and details of tension compression test have been reported. A numerical scheme has been developed to determine the strain increment for given stress increment using given material constants. Simulated results are compared with the experimental data and are found to be in good agreement.

Keywords : *fire, viscoplastic, high temperature*

1. INTRODUCTION

Recently there has been considerable interest in developing so called 'unified' elastic viscoplastic constitutive equations. A unified model differs from a non-unified model in its basic assumptions. In a non-unified model, the contributions of elastic, plastic and creep strain increments to total strain increment are considered to be uncoupled and independent for simplification. Thus each component is calculated separately using different principles and then added to give the total strain increment. However, in a unified model, although elastic and inelastic strain increments are separated, the inelastic part is assumed to represent all aspects of inelastic deformation. Thus the real phenomena, like plasticity-creep interaction, can be more accurately expressed. The basic purpose of the present work is to develop a constitutive model that can be used to predict the response of civil and architectural structures in fire environments. Earlier works by Baba et al. were based on a non-unified concept[1)~6)]. At that time the unified model concept was not fully developed and a non-unified model was the only well established method applicable to a combined rate and time dependent material. Consequently, extension to a unified model was considered as a future work. The present work is in connection to that work.

The deformation of steel under a fire environment is both rate and time dependent. These rate and time dependencies can be explained using Fig.1. The variation of stress-strain behavior with time is represented by a σ-ε-t surface (**Fig.1**(a)). If the surface is cut vertically, passing through the origin, it will represent the tensile test (**Fig.1**(b)). The section of the σ-ε-t surface in σ-ε plane will represent a tensile test for infinite strain rate. This means that the loading process is completed in zero time, hence, there is no time for creep to occur. The shape of this curve represents rate dependency. If the σ-ε-t surface is cut by a horizontal plane at any stress level, creep test curve at that stress level can be obtained (**Fig.1**(c)). This creep curve represents time dependency. Currently available unified viscoplastic models are suitable for either of these dependencies. For instance, the Bodner-Partom model[7)] is quite suitable to predict strain rate dependency, but it is not a proper choice to represent time dependent phenomena like creep. Similarly, Miller[10)] based his model basically on stationary creep. Thus time dependency has been taken into account but rate dependency has not been considered. Even for the time dependency, his model does not properly reflect non-stationary time dependent phenomena like transient creep.

The main purpose of this study is to develop a constitutive model, which is equally suitable for the prediction of both rate and time dependencies, and their interaction, because they are the major characteristics of material behavior under fire environment. Moreover the model should be capable of covering non-stationary creep. Although, the model presented here is of unified type, but authors prefer to call it 'semi-unified model'. The reason for using the prefix 'semi' is explained in section 2.

* Member of JSCE, M. Eng., Graduate Student, Department of Civil Engineering, Nagoya University (Furo-cho, Chikusa-ku, Nagoya 464-01).
** Member of JSCE, Dr. Eng., Associate Professor, Department of Civil Engineering, Nagoya University

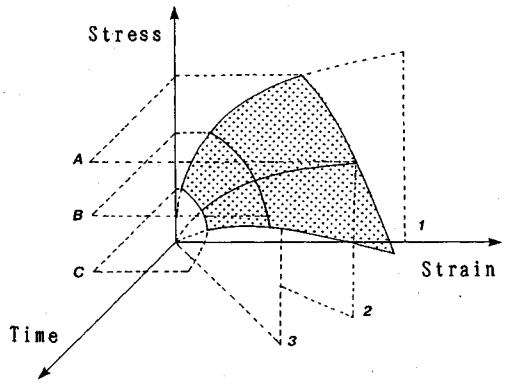

Fig.1(a) σ-ε-t surface

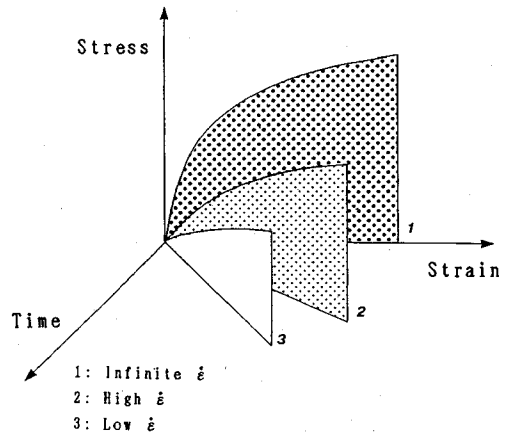

Fig.1(b) Tensile test (rate dependency)

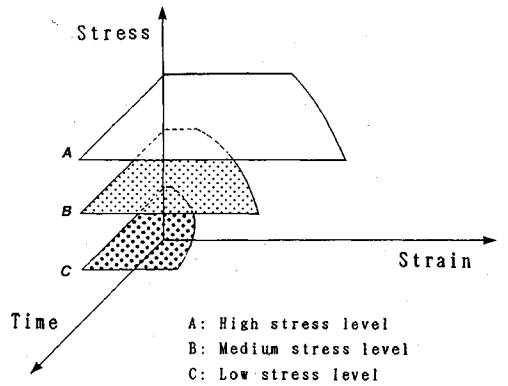

Fig.1(c) Creep test (time dependency)

2. MATHEMATICAL FORMULATION

(1) Physical Concept

It is assumed that the total strain increment tensor $d\varepsilon$ can be additively decomposed into its elastic $d\varepsilon^e$ and inelastic $d\varepsilon^{in}$ components

$$d\varepsilon = d\varepsilon^e + d\varepsilon^{in}$$

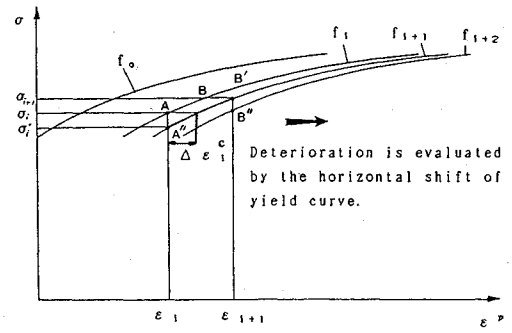

Fig.2 σ-ε^p curve. The effect of time dependency is introduced by shifting the curve to the right (tensile loading)

The elastic part is calculated using Hooke's law. As is explained earlier, since the present model is developed with the intention of using it to predict the response of civil and architectural structures in fire conditions, it is important to account for both rate and time dependencies of deformation and their interaction. These phenomena are considered major factors in a fire environment. Thus the inelastic strain increment will include strain rate effects as well as time dependent effects. The shape of the effective stress-effective plastic strain ($\bar{\sigma}$-$\bar{\varepsilon}^p$) curve, obtained from the experimental data itself will reflect the strain rate effects. Thus rate effects can be calculated from the experimental data. Time dependent effects will be taken into account by considering a contraction in the yield surface. This contraction of yield stress, termed 'deteriorated stress' will be evaluated by giving a horizontal shift to the $\bar{\sigma}$-$\bar{\varepsilon}^p$ curve at each step of loading, as shown in **Fig.2**. It is assumed in the present model that the amount by which the curve shifts is equal to creep strain produced during that loading step. As only creep is used to consider the effect of time dependency, the present model can be called a semi-unified model.

(2) Constitutive Law

Assuming the von Mises yield criterion and isotropic work hardening, yield function f^* can be represented as

$$f^* = f - \sigma_y(\bar{\varepsilon}^p)$$

where $f=\bar{\sigma}$, $\bar{\sigma}$ is the effective stress and $\bar{\varepsilon}^p$ is the plastic strain tensor. We have the Prandtl-Reuss equation defined as

$$d\varepsilon^p = (3\Lambda/f)\boldsymbol{s} \quad \cdots\cdots (1)$$

In classical theory of plasticity, Λ is defined as a positive scalar factor which represents the magnitude of plastic strain increment and $\boldsymbol{s}$ is the deviatoric stress tensor. Using Prager's consistency condition $df=0$, Λ can be determined as

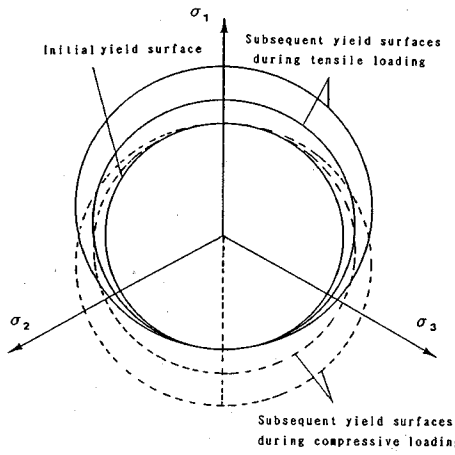

Fig.3 Representation of hardening in the π-plane

$$\Lambda=\frac{(\partial f/\partial\boldsymbol{\sigma}) : \boldsymbol{E}d\boldsymbol{\varepsilon}}{H+(\partial f/\partial\boldsymbol{\sigma}) : \boldsymbol{E}(\partial f/\partial\boldsymbol{\sigma})} \quad \cdots\cdots (2)$$

where $\boldsymbol{\sigma}$ and $\boldsymbol{\varepsilon}$ are the stress and strain tensors respectively, H is the slope of the effective stress-effective plastic strain (i.e., $\bar{\sigma}$-$\bar{\varepsilon}^p$) curve and $\boldsymbol{E}$ is the elastic stiffness tensor.

(3) Creep Effect Calculation

As explained earlier the effect of time dependency will be taken into account in the form of contraction of yield surface. This idea can be considered as a special case of isotropic recovery theory[9]. This reduction of yield stress can be calculated by giving a horizontal shift to the $\bar{\sigma}$-$\bar{\varepsilon}^p$ curve (right side for tensile and left side for compression) by an amount equal to the creep strain resulting during the time taken by the load to increase from $\bar{\sigma}$ to $\bar{\sigma}+d\bar{\sigma}$. In **Fig.2** f_0 represents original $\bar{\sigma}$-$\bar{\varepsilon}^p$ curve, and f_i, f_{i+1} and f_{i+2} represent the subsequent $\bar{\sigma}$-$\bar{\varepsilon}^p$ curves shifted to the right in order to evaluate the deteriorated stresses. AA'' and BB'' are the stress reduction at time steps i and $i+1$ respectively. For i-th step the deteriorated stress is given by :

$$\bar{\sigma}_i^*=f_0(\bar{\varepsilon}_i^p-\sum_{j=1}^{i}\Delta\bar{\varepsilon}_j^c) \quad \cdots\cdots (3)$$

where $\Delta\bar{\varepsilon}_j^c$ is the corresponding effective creep strain of time step j.

(4) Modification of Hardening According to the Experimental Evidence

During the experimental work, described later, it was found that SS 41 steel, which was used for the experiments, shows some special characteristics in the hardening pattern. If the specimen is loaded in tension in the plastic region, the yield surface starts expanding. Now, if the specimen is unloaded and reloaded in tension, deformation is fully elastic. However, if the strain exceeds the previous maximum strain, the plastic deformation occurs and yield surface begins to expand again. The specimen shows similar behavior in compression. The most interesting feature is that every time the loading is reversed from tension to compression or compression to tension, the material starts yielding at the initial yield value. This phenomenon, discovered during the uniaxial tension compression test, can be extended to the three dimensional π-plane as shown in **Fig.3.**

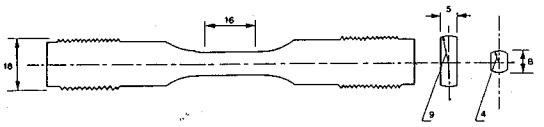

Fig.4 The specimen. All dimensions are in mm

3. EXPERIMENTAL DETAILS

The material tested was SS 41 steel, which is an ordinary structural steel in Japan. The experimental program was accomplished in two phases.

(1) Creep Test

In the first phase, a series of tensile creep tests controlled under constant true stress were performed and have already been reported[2)~6)]. The test results were used to represent the transient creep in the form of functions, in which the technique of spectrum decomposition based on the generalized Voigt type rheology model was used. The same functions are used in the present work to evaluate the effect of creep, except that small modifications are made in some parameters, which will be explained in the next section.

(2) Tension Compression Test

The second phase of the experimental work was performed quite recently. Double cycle tension compression tests were carried out on specimens cut in the longitudinal direction from the web of rolled H-beam. This is the reason for the noncircular cross section of the specimen (**Fig.4.**).

The same beam was used to make specimens for the creep test. The tests were carried out at temperatures of 300, 400, 450, 500, 550, 600, 650 and 700°C.

a) Experimental Apparatus

The load frame used in these tests, was an MTS electro hydraulic test machine. An MTS 661. 23 B-01 25 ton load cell was used as the load transducer. A high temperature displacement transducer of type HDP-05-16, made by Tokyo Sokki Kenkyujo, was used to measure the strain. The displacement was measured for specific length of the central part of the specimen. The transducer was attached to the cylindrical surface of the specimen in the longitudinal direction. An electric furnace made by

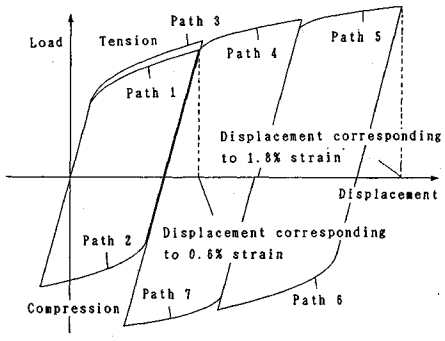

Fig.5 Loading program

Toshin Kogyo, type Kantaru A-1-2 and thermocontroller with 0.5 percent accuracy were used for temperature control. Three thermocouples were attached at the upper, central and lower parts of the specimen to check the temperature control. Thermocouples were covered with asbestos thread to avoid the radiation of the surrounding furnace walls.

b) Loading Program

Initially, some tests were conducted under stroke control at a strain rate of 0.1% per minute. The creep effect was so dominant that hardening characteristics were not clear. Hence the control was changed to load control. Loading rate was controlled manually. For each interval of loading, load for each 2 second time interval was recorded and creep strain component was calculated for each time step separately. Strain rate during elastic region was approximately between 0.2 to 0.4%/min. While during plastic region it was approximately between 1.5 to 3.0%/min. Loading was applied in two cycles, each of initial tension followed by compression. A typical loading plan is shown in **Fig.5**. The first cycle was a complete cycle. Path 1 was tension and path 2 was compression. In the second cycle, the tensile loading was applied following path 3, 4 and 5 while compressive loading through path 6 and 7. In this cycle the loading was removed before completing the full cycle. The reason for terminating the test at this point was that the data necessary for model had already been obtained. In order to prevent the buckling of the specimen during compression, the buckling load was calculated before the test and care was taken to keep loading below the buckling load of the specimen. Load-time as well as Load-displacement data were recorded automatically through a micro-computer.

c) Use of Test Data

The load-displacement data obtained from the experiment is first converted to stress-total strain data. Creep strain component produced during each step of loading is estimated using Corum's model[8]. The creep and elastic strain components are subtracted from the total strain to get instantaneous plastic strain component, which finally gives $\bar{\sigma}$-$\bar{\varepsilon}^p$ curve. This curve is used to determine model parameters explained below.

4. DETERMINATION OF MATERIAL CONSTANT FROM TEST DATA

Values of the material parameters for SS 41 steel are determined from constant stress creep tests (spanning the ranges of temperatures and stress levels) and tension compression tests (performed at the same temperatures as creep test) by following the procedure outlined below.

(1) Creep Test

Using the concept of retardation spectrum based on a four element Voigt model, uni-axial, creep curves obtained from the test data are represented in the form of a function given as follows.

$$\varepsilon^c = J_1(1-\exp(-t/T_1)) + J_2(1-\exp(-t/T_2)) \quad \cdots\cdots (4)$$

in which J_1 and J_2 are nondimensional compliances, T_1 and T_2 are retardation times and t is time in minutes. In the previous work these parameters were expressed as logarithmic functions. As the tension compression tests were conducted at a very high strain rate, the specimen could take large stresses at high temperatures. It was not possible to apply such large stresses at high temperatures for a long period in the creep test. Very soon the material underwent accelrated straining. Extrapolation for such large stresses, using logarithmic functions does not give a good approximation. Thus the functions are modified as follows :

$$J_1 = (C_{J1}\sigma^c + D_{J1})^2$$
$$J_2 = (C_{J2}\sigma^c + D_{J2})^2$$
$$T_1 = (C_{T1}\sigma^c + D_{T1})^2$$
$$T_2 = (C_{T2}\sigma^c + D_{T2})^2$$

where $C_{J1} \sim C_{T2}$ are functions of temperature. Typical values are shown in Table 1. σ^c is the constant true stress used in the creep test. Eq.4 is used to determine the corresponding creep used in Eq.3.

(2) Tension Compression Test

From the tension compression test data, creep and elastic components are subtracted to get the $\bar{\sigma}$-$\bar{\varepsilon}^p$ curve (**Fig.6**). The strain hardening is represented by the following equation :

$$\bar{\sigma} = C\bar{\sigma}_0 + A_1(1-\exp(-\bar{\varepsilon}^p/B_1)) + A_2(1-\exp(-\bar{\varepsilon}^p/B_2)) \quad \cdots\cdots (5)$$

where σ_0 is the initial yield stress, A_1, B_1, A_2, B_2 and C are functions of temperature and are determined by best fit to the $\bar{\sigma}$-$\bar{\varepsilon}^p$ curve obtained from the test

Table 1 Material Parameters for SS 41 Steel (creep test)

temp °C	C_{J1} $\frac{mm^2}{kg}$	D_{J1} –	C_{J2} $\frac{mm^2}{kg}$	D_{J2} –	C_{T1} $\frac{min^{\frac{1}{2}}\text{-}mm^2}{kg}$	D_{T1} $min^{\frac{1}{2}}$	C_{T2} $\frac{min^{\frac{1}{2}}\text{-}mm^2}{kg}$	D_{T2} $min^{\frac{1}{2}}$
300	0.0030	-0.050	0.0028	-0.061	0.021	0.0030	0.030	1.83
400	0.0016	0.0062	0.0064	-0.11	0.016	0.46	0.095	1.80
450	0.0044	-0.050	0.011	-0.15	0.020	0.55	0.080	3.30
500	0.0044	-0.025	0.025	-0.285	0.080	-0.15	0.40	-0.25
550	0.0072	-0.042	0.055	-0.45	0.050	0.38	0.42	1.90
600	0.0080	-0.025	0.15	-0.92	0.080	0.27	0.84	2.80
650	0.012	-0.030	0.35	-1.30	0.015	1.00	1.70	5.50
700	0.011	-0.015	0.90	-2.10	0.120	0.70	3.20	8.80

Table 2 Material parameters for SS 41 Steel (tension compression test)

temp °C	σ_0 $\frac{kg}{mm^2}$	A_1 $\frac{kg}{mm^2}$	B_1 –	A_2 $\frac{kg}{mm^2}$	B_2 –	C –
300	15.0	17.00	.0070	5.00	.00040	1.080
400	12.0	14.00	.0060	4.20	.00050	1.070
450	10.0	12.60	.0053	4.00	.00030	1.046
500	9.0	8.50	.0050	5.00	.00030	1.000
550	8.0	6.50	.0050	3.75	.00040	0.960
600	7.0	4.30	.0050	2.70	.00050	0.930
650	5.0	2.20	.0052	3.30	.00040	0.910
700	3.0	2.40	.0050	2.80	.00040	0.820

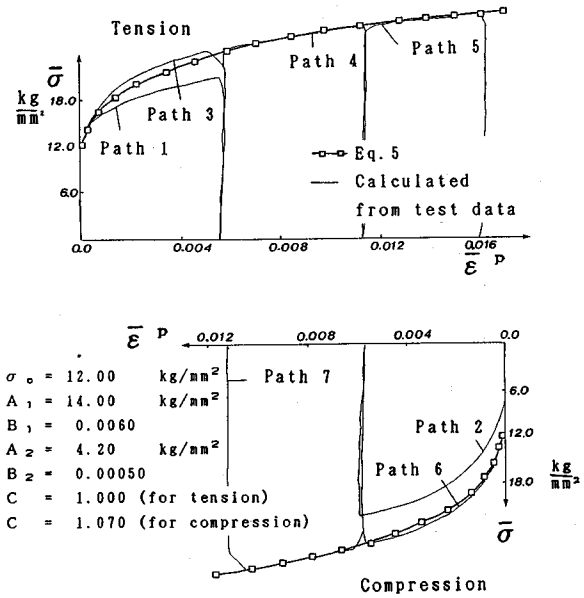

Fig.6 Calculation of the model parameters from the test data (400°C case)

data. Typical values are shown in Table 2. An exponential function is selected because it is easy to take a derivative and it resembles the creep equation.

5. NUMERICAL SCHEME AND COMPARISON OF SIMULATION WITH EXPERIMENTAL DATA

(1) Numerical Scheme

A numerical scheme is devised to determine the strain increments at each stage of loading for the given material constants at a specified temperature. The scheme is applied to trace the experimental data of the tension compression tests. The specimen is modeled by a 3-node, 3-degrees of freedom bar-element. Three Gaussian points are used for numerical integration. A nonlinear iterative solution is obtained using modified Newton-Raphson method while stiffness is determined by the displacement method.

(2) Comparison of simulation with experimental data

The predictive capability of the model is checked

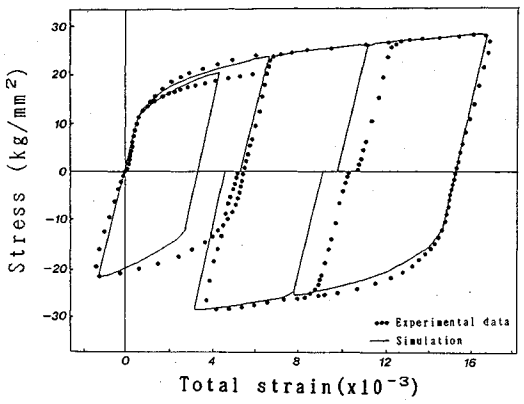

Fig.7 Stress strain relations. Comparison of experimental data with the simulation (400°C)

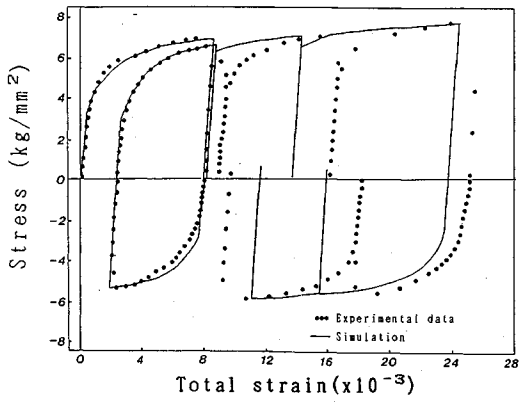

Fig.8 Stress strain relations. Comparison of experimental data with the simulation (700°C)

by comparing the simulated results with the experimental data for all temperature cases. Two typical cases are presented here, one at medium-low temperature (400°C) and one at medium-high temperature (700°C). **Fig.7** shows the response of the model as compared to the test data at 400°C for a loading history explained previously.Simulated calculation shows good agreement with the test data. For the first cycle the strains calculated by the model are less than the measured values. On the other hand, the model shows good agreement for the second cycle. This effect can be attributed to the isotropic hardening which is more pronounced at lower temperatures.

Fig.8 shows the comparison for a similar loading history at 700°C. Model results show good agreement with the test data, except small discrepancies appear on the unloading path. This is partly due to the fact that the tests were performed on load control. Moreover, as this model is specifically made for the fire analysis of civil and architectural structures, only one cycle (heating followed by post fire cooling) is expected. Thus this effect can be neglected.

6. CONCLUSIONS

The following conclusions have been made :

(1) A semi-unified constitutive model for elastic viscoplastic material at high temperature has been developed.

(2) Material constants necessary for the model can be obtained by the standard laboratory creep and tension compression tests.

(3) SS 41 steel is tested and predicted values compared with the actual test data show good agreement.

(4) Extension for multidimensional stress state is possible.

The resistance and the safety of civil and building engineering structures during and after fire will be discussed in our next report.

ACKNOWLEDGMENTS

The contributions of Mr. Shahid, Mr. Iwamoto, Mr. Kanza and Mr. Yabunaka in conducting the experimental work are gratefully acknowledged.

REFERENCES

1) Baba, S. and Yamamoto, T. : Strength of Steel Frame Structures in Fire, Proc. IABSE Symp. on Strengthening of Building Structures. Venezia. pp.243～250, 1983.

2) Baba, S. and Nagura, H. : Effect of Material Properties on the Deformation of Steel Frame in Fire, Proc. JSCE Structural Eng./Earthquake Eng., Vol.2.1, pp.47～57, 1985.

3) Baba, S. and Segi, K. : Formulation of High Temperature Creep and its Application to the Structural Analysis (in Japanese), Proc. 9 th Symp. on Computational Methods in Structural Eng. and Related Fields. Tokyo, pp.139～144. 1985.

4) Baba, S. and Nakada, N, : Time Dependent Deformation of Steel Structures in Fire, Proc. 3rd Int. Conf. on Numerical Methods For Non-linear Problems, Dubrovnik, pp.536～549, 1986.

5) Baba, S. and Nakada, N, : Steel Frame Structures in Fire-Effect of Creep and Work Hardening Proc. of the Int. Conf. on Steel Structures, Budva, pp.89～97, 1986.

6) Baba, S. Nakada, N.and Segi, K. : Deformation and Strength of Steel Frame Structure in Fire Environments, (in Japanese), Proc. JSCE. No.380/1-7, pp.303～310, 1987.

7) Bodner, S. R. and Partom, Y. : Constitutive Equations for Elastic Viscoplastic Strain Hardening Materials, ASME Journal of Applied Mechanics, pp.385～389, 1975.

8) Corum, J. M., Greenstreet, W. L., Liu, K. C., Pugh, C. E. and Swindeman, R. W. : Interim Guidelines for Detailed Inelastic Analysis of High-Temperature Reactor System Components, Oak Ridge National Laboratory, ORNL-5014 (1974)

9) Ioue, T. : On the Inelastic Constitutive Relationships under Plasticity-Creep Interaction with the Application to Cyclic Behavior and the Methods of Life Prediction under Fatigue-Creep Intercation, Journal of the Society of Materials Science, Japan, Vol.32, No.357, pp.594～604, 1983.

10) Miller, A. K. : An Inelastic Constitutive Model for Monotonic, Cyclic, and Creep Deformation, Part I, Equations Development and Analytical Procedures, Part II, Application to Type 304 Stainless Steel. ASME Journal of Engineering Materials and Technology, Vol.94, pp.97～113, 1976. **(Received November 22, 1990)**

高温時の弾-粘塑性材料に対する準統合化モデル

SYED Saeed Ahmad・馬場俊介

火災時のような急速昇温現象に対しては，クリープの大量発生（粘性）と降伏点の急低下（塑性）が同時に進行するため，従来の粘塑性統合化モデルでは取り扱うことができない．本論文では，クリープを降伏面の縮小で置換して（近似的に）塑性に組み込むという準統合化モデルを提案する．本文中には，モデルの定式化と，高温引張圧縮実験結果の紹介と，モデルの適合性への検証を含む．